ATTENUATION IN CONCRETE OF A NEUTRON FLUX EMITTED AT AN ANGLE OF 90° TO THE PRIMARY PROTON BEAM OF A 10 Gev SYNCHROPHASOTRON

V.E. Aleĭnikov et al.

Translated by R.F. Zobel (December 1966) from the Russian Oslablenie v betone potoka neĭtronov ispuskaemykh pod uglom 90° k napravleniyu pervichnogo puchka protonov sinkhrofazotrona na 10 Gev. Joint Institute for Nuclear Research Preprint 9-2933. Dubna 1966, 14 pp.

TRANSLATED FOR

STANFORD LINEAR ACCELERATOR CENTER

ATTENUATION IN CONCRETE OF A NEUTRON FLUX EMITTED AT AN ANGLE OF 90° TO THE PRIMARY PROTON BEAM OF A 10 Gev SYNCHROPHASOTRON

V.E. Aleĭnikov, V.N. Lebedev, V. Mantseva, and M.I. Salatskaya

In the planning of protective shielding for proton ring high-energy accelerators one often comes across the kind of arrangement shown in Figure 1. The source of the radiation and the shielding are then so disposed that radiated flux emitted at an angle $\Theta = 90^{\circ}$ to the primary proton beam which is bombarding the target is incident on the plane on the shielding. Very little is known about the output and the spectral distribution of this flux, and therefore estimation of the necessary thickness of shielding a priori is difficult. The purpose of the present work was thus to obtain the lacking information on the attenuation of nucleon and meson flux in concrete shielding disposed as shown in Figure 1, and

to compare the results with calculations based on reasonable simplifying assumptions about the form of the spectral and angular distributions.

Principal characteristics of the secondary radiation

Nucleons and mesons were generated at a 20 x 40 x 160 mm beryllium target or at a 30 x 30 x 90 mm copper target, placed within the vacuum chamber of the OIYaI /JINR/ synchrophasotron, in the rectilinear receptacle cavity. Beryllium was chosen as a target because the spectral distribution of the secondary particles has been quite well studied for beryllium. Copper was used mainly on the basis of practical considerations, since the main circuitry and components of the accelerator onto which the proton flux is deflected at the end of the accelerator cycle, are made of materials of medium atomic numbers such as copper, iron, or stainless steel.

Spatial - angular distribution.

The space distribution of secondary nucleons and π-mesons generated at the target was determined experimentally under various conditions: in the arrangement shown in Figure 1 when the target was virtually outside the

magnetic field, and also when it was inside the vacuum chamber between the poles of the electromagnet. In both cases the detector of the high-energy particles was a threshold activated detector on a C^{12} base ($E_{\text{nucleon threshold}}$ = 20 Mev, $E_{\tilde{\pi}\ \text{threshold}}$ = 50 Mev). The space distributions of the secondary particles measured in this way are given in Figure 2. It should be mentioned that these distributions were not obtained under ideal conditions, since in particular, the influence of the vacuum chamber walls and of the magnetic field on the trajectory of the charged particles was not included. However, these effects are estimated to be small and the spatial distributions obtained may be approximately interpreted as angular. Moreover, it is desirable in working out biological and technological shielding for the given accelerator to have the distribution of the secondary particles measured under just such conditions.

The experimentally determined yield of secondary components (n, p, $\tilde{\pi}^{\pm}$) into a solid angle of $3.73\tilde{\pi}$ along the direction of the beam (which corresponds to an angle of 150° between the directions of the primary protons and the liberated secondary particles) is equal to 3.5 ± 0.5 particles per

accelerated proton for a copper target and 2.3 $\pm$ 0.5 for a beryllium target. Since we have no accurate knowledge of the effectiveness of the targets used, it is difficult to reach a sound conclusion regarding the absolute value of the yield per interacting proton. On the supposition that all the protons eventually pass through the region of the target, which is close to reality, the effectiveness of the copper and beryllium target is respectively 0.4 and 0.3.

Since it is possible that the circulating protons will miss the target or pass through only a part of it, it is clear that the true yield will be somewhat greater, i.e.

$$B_{Cu} > 9 \qquad\qquad B_{Be} > 7.5.$$

In comparison with published data, in particular the estimates carried out by empirical formulas given in ref. 1, based on extensive factual material ($B_{Cu} = 5.4$ and $B_{Be} = 4.3$ for slower particles), the yields found by us are evidently too small by a factor of ~ 2 if we take into account the low recording threshold of our detector.

The results shown in Figure 2 are described by an empirical relation-

ship of the form $k\ (\theta + \theta_o)^{-n}$. The values of k, θ, and n are given in Table 1 in relation to target materials; the normalizing factor k is given on the basis of a total yield of 10 nucleons per proton.

Table 1.

Target material	θ_o	k	n
Copper	0.157	1.2	1.6
Beryllium	0.175	1.14	1.8

The errors indicated in the figure include both those due to the apparatus and those due to the indeterminate nature of the effect of protons deflected onto the walls of the vacuum chamber of the accelerator. This effect is greatest for $\theta > 90^o$, when the particle flux from the target becomes comparable in order of magnitude with that generated at the walls.

The same figure also shows, for purposes of comparison, angular and spatial distributions of secondary components obtained by other workers. Curve 2 of Figure 2a shows the angular distribution of neutrons from a thick copper target bombarded with 6.3 Gev protons[2]. Curve 2 in Figure 2b was obtained experimentally by bombardment with 10 Gev protons[3]. In the

latter instance the method of measurement was the same as ours, except that in ref. 3 the target was "thin" and was situated outside the magnetic field. This should be taken into consideration when comparing the curves, since the presence of the magnetic field leads to a slight broadening of the angular distribution curve.

Composition and spectral distribution

The expected distribution of secondary particles (π -mesons and nucleons) generated at a target at an angle of 90° to the direction of the primary 10 Gev protons is given in Figure 3. This distribution was obtained on the assumption that the fluxes of secondary particles may be interpreted as a combination of two independent distributions of transverse momenta p_1 and longitudinal momenta p_2, i.e.

$$f(p_1, p_2)dp_1dp_2 = g_1(p_1)dp_1 \cdot g_2(p_2)dp_2 ,$$

where $f(p_1, p_2)$ is the probability of the formation of particles with transverse momentum p_1 and longitudinal momentum p_2; $g_1(p_1)$ and $g_2(p_2)$ are functions of the spectral distribution of the transverse and longitudinal momenta of the secondary particles.

We further assumed that the transverse momentum distribution $g_1(p_1)$ of the secondary particles does not depend on the energy of the primary particles, which is not in disagreement with the experiments[4] for proton energies ranging from a few to 10^4 Gev, and consequently the spectrum of secondary particles emitted at an angle of 90° to a target bombarded by 10 Gev protons is identical with the spectrum in the case of bombardment with 29.5 Gev protons[5] (Curves 1 and 2 in Figure 3).

For comparative purposes Figure 3 also shows the experimental spectrum of neutrons generated in a lead target by 10 Gev protons at an angle of 90° to the direction of the primary protons[6].

It follows from examination of the spectra presented here that nucleons and mesons with an energy of the order of several tens or hundreds Mev are liberated from the target at an angle of 90° to the incident beam. The flux of particles rapidly decreases with increasing energy. Of these particles, only the neutron component has any significance because a large part of the protons and π-mesons is absorbed by the walls of the vacuum chamber and does not reach the shielding. Moreover, ~50% of the π-mesons disintegrate as they travel over the 8.35 m separating the target and the

shielding. Analysis of the nuclear interactions in emulsions placed on the surface of the shielding gives a ratio between the stars formed by the neutral and the charged components in conformity with the above statements, i.e.

$$N_{neutral}/N_{charged} = 20.$$

The problem of the value of the μ-meson flux remains open. However, it is not necessary to be precise about this value, because the energy of μ-mesons is low and they are completely absorbed at a depth of the order of 1-1.5 m of concrete.

Results and discussion

Figure 4 shows particle flux densities (primarily of neutrons) in concrete (ρ = 2350 kg/m^3) at various depths, obtained with the threshold detector working on the principle of the measurement of radiation-induced activity of C^{11} in a liquid scintillator. The measurements were carried out for three energies of the internal beam of protons: 10, 7, and 3.2 Gev. The results for these energies agree within the limits of experimental error. This is evidently due, as mentioned earlier, to the fact that the

spectrum of secondary particles emitted at 90° from the target is virtually independent of the energy of the primary particles in this range of energy, and the mean multiplicity of nucleons in the energy range 3-10 Gev varies only slowly[7]. The figure shows also, for comparative purposes, a computed curve for the attenuation of neutrons with an energy of $\geq$ 20 Mev. In calculating this curve it was assumed that the rate of attenuation of the flux of such neutrons is determined mainly by the rate of attenuation of the flux of neutrons with an energy exceeding 80 Mev[8]. The computations were performed using the solution (obtained in ref. 8) of the kinetic equation for a monodirectional monochromatic neutron flux incident normally on a semi-infinite absorber, without allowance for the angular scattering of neutrons resulting from interaction with nuclei:

$$\Phi(x) = e^{-\mu x} I_0\left(2\sqrt{\eta \mu x (E_0 - E_1)}\right) \qquad (1)$$

where $\Phi(x)$ is the neutron flux at depth x with energy in excess of E_1 = 80 Mev, $\mu = 2.27 \times 10^{-2}$ cm^{-1} is the linear attenuation coefficient of the neutrons, equal to $n_0 \sigma_{in}$ (where σ_{in} is the cross-section of inelastic interaction between neutrons and nuclei and n_0 is the number

of nuclei in 1 cm^3 of the absorber); $I_o\left(2\sqrt{\eta\mu x(E_o-E_1)}\right)$ is the Bessel function of zero order of imaginary argument; E_o is the energy of the primary neutrons.

The coefficient η may be represented by:

$$\eta=\nu(E')f(E)A(E'),$$

where $\nu(E')$ is the mean multiplicity of secondary neutrons formed during an inelastic interaction of a neutron having an energy E' with a nucleus; $f(E)$ is the spectrum of secondary neutrons; $A(E') = \left[\int_{80}^{E'} f(E)dE\right]^{-1}$ is the normalizing factor.

Since the solution of the kinetic equation which we have adopted is correct only when η = const, the calculation of the attenuation curve was made by choosing for $\nu(E')$ and $f(E)$ mean values in the energy interval of 80-200 Mev. Curve 2 in Figure 3 shows the neutron spectrum used in the calculation.

The spectrum was normalized to the particle flux density measured by the threshold carbon detector at a point in front of the shield (x = 0). The attenuation curve in Figure 4 was computed for E_1 = 80 Mev and

$\eta = 2.8 \times 10^{-3}$ Mev^{-1}. As may be seen, there is good agreement between the calculated curve and the experimental results. Figure 4 also shows the results of measurements of the flux density of neutrons with an energy of < 20 Mev at different depths of concrete. These measurements were obtained by means of a "long", BF_3-filled, proportional counter.

Comparison of the attenuation curves for nucleons with $E > 20$ Mev and neutrons with $E_n < 20$ Mev at depths in concrete greater than 100 cm (i.e. where there are virtually no primary particles) shows that the mean neutron accumulation factor for $E_n < 20$ Mev is equal to 2.

Apart from measuring nucleon flux densities in the shielding, we also irradiated nuclear emulsions of the 'p' type. Figure 5 gives measured star densities at various depths in the concrete. It also shows a calculated curve showing the relationship between the neutron star density and thickness of the concrete, calculated from equation (1). The threshold of star formation was taken as 80 Mev, $\eta = 2.8 \times 10^{-3}$ Mev^{-1}, and the spectrum of primary neutrons was normalized to the density of neutron stars at a point in front of the shield ($x = 0$). The cross-section for star formation was taken as independent of the neutron energy.

It follows from Figures 4 and 5 that the attenuation law for the neutron fluxes may be taken as exponential. Table 2 shows the half-value layer thicknesses ($\Delta_{\frac{1}{2}}$) obtained by us for the secondary particle fluxes in concrete (ρ = 2350 kg/m^3). For comparison, the table shows also $\Delta_{\frac{1}{2}}$ values for energies of 0.17-0.66 Gev as given by Komochkov and Sychev[8].

Table 2.

Energy of primary protons Gev	Direction of the beam of secondary particles	Method of measurement	$\Delta_{\frac{1}{2}}$	
			expt.	calc.
0.170	0°	threshold detector	29 ± 2	33 ± 2.6
0.250	0°	dto.	34.5 ± 2	36 ± 2.9
0.350	0°	dto.	38 ± 2	38.5 ± 3.1
0.480	0°	dto.	43 ± 3	41 ± 3.3
0.660	0°	dto.	42 ± 1	42.3 ± 3.3
3.2	90°	dto.	45 ± 2	43.5
7.0	90°	dto.	45 ± 2	43.5
10.0	90°	dto.	45 ± 2	43.5
10.0	90°	"long" counter	44 ± 2	43.5
10.0	90°	Nuclear emulsion	50 ± 4	43.5

It will be seen from Table 2 that the thicknesses of the secondary radiation half-value layers in concrete which we have obtained are close to the values of $\Delta_{\frac{1}{2}}$ for secondary radiation emitted at 0° to the primary beam in a 660 Mev synchrocyclotron[8]. However, in our geometrical layout there is practically no transition region on the attenuation curves (Figures 4-5),

which is in good agreement with the spectrum of the incident neutrons (Figure 3).

The data given above enable one to compute fully the lateral shielding for the JINR synchrophasotron, assuming with an accuracy sufficient for practical purposes that the exit* cross-section of very fast particles for ordinary concrete (ρ = 2350 kg/m^3) is equal to

$$\Sigma_{rem} = 0.65 \times 10^{-3} \text{ m}^2/\text{kg}$$

The results obtained clearly may also be used for planning the lateral shielding of high-energy proton ring accelerators (up to hundreds of Gev), since the spectra of secondary particles emitted at an angle of 90° to the target, as previously stated, depend little on the energy of the primary protons in this energy interval.

The authors are indebted to V.S. Sychev for valuable criticism.

R e f e r e n c e s

1. W. Yucker, Transact. of the Am. Nucl. Soc. 8 (1965) 632.
2. B. Moyer, Premiere Colloque International sur la Protection Aupres des Grands Accelerateurs, p. 65 (Presses Universitaires de France, Paris, 1962).

---

* Translator's note: ?

3. L. Hoffman and A. Sullivon Nucl. Instr. and Methods 32 (1965) 61.
4. Cocconi G., Fluxes of Secondary Particles from Ultrarelativistic Proton Accelerators. Ithaca, 1961 (Cornel. Univ.).
5. R.L. Cool, Proceedings of the Brookhaven International Conference on High Energy Accelerators (Sept. 1961) p. 15.
6. M. Anikina et al., JINR Preprint P-2065, Dubna 1965.
7. V.S. Barashenkov et al., JINR Preprint P-2393, Dubna 1965.
8. M.M. Komochkov and B.S. Sychev, JINR Preprint 1167, Dubna 1963.

Submitted September 19, 1966.

oooooooooooooooo

Translation supplied by

Fig. 1.

Experimental arrangement

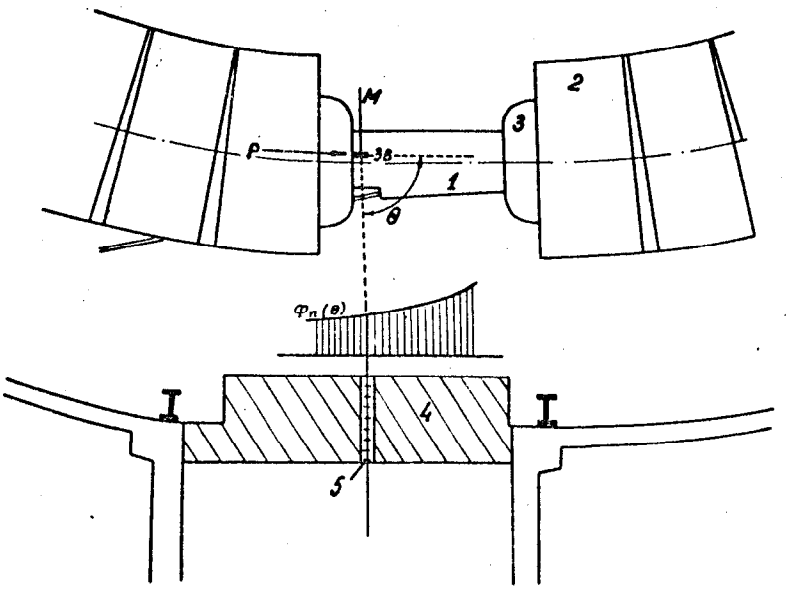

Key:

1. rectilinear interval
2. yoke of synchrophasotron electromagnet
3. winding
4. concrete shielding
5. experimental installation
M. target
p. direction of the proton beam

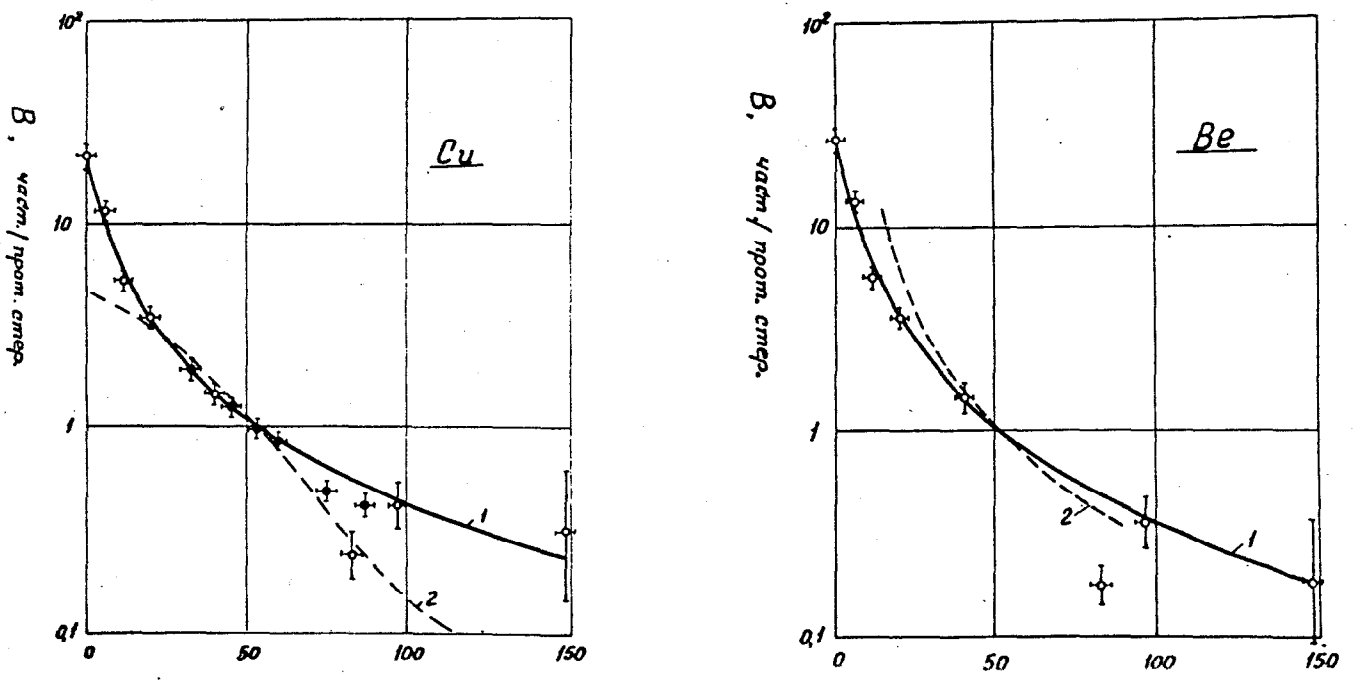

Fig. 2. Spatial distribution of nucleons with energy in excess of 20 Mev and π-mesons with energy exceeding 50 Mev. a. Copper target; •o experimental points; 1. function of the form $k(\theta + \theta_o)^{-n}$; 2. angular relationship derived by Moier[2] for primary 6.3 Gev protons; b. Beryllium target: o experimental points; 1. function of the form $k(\theta + \theta_o)^{-n}$; 2. angular relationship found experimentally[3] for thin targets when the energy of the primary protons is 10 Gev.

Ordinates: B, particles/proton. sterad; Abscissae: θ, degrees

Figure 3. Energy spectrum of neutrons emitted at right angles to a target of material with a moderate atomic number.

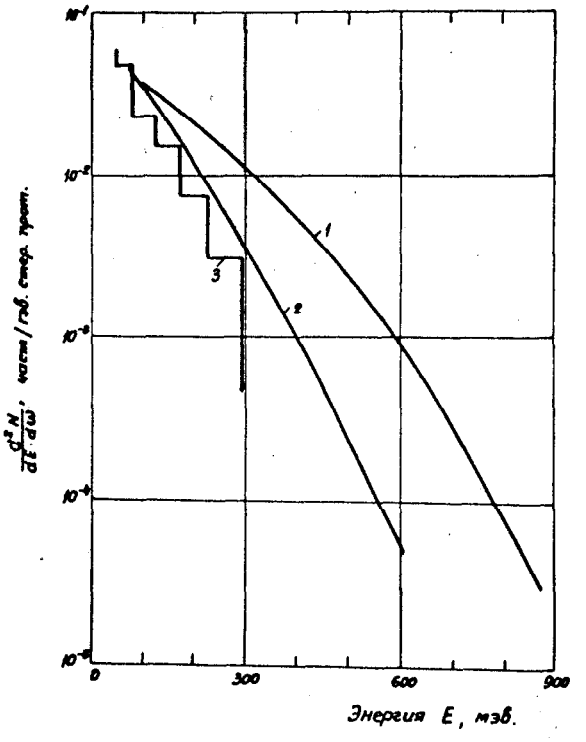

1. π^--mesons and a Be target[5]
2. protons and a Be target[5]
3. neutrons and a Pb target[6]

The curve is normalized to facilitate comparison

Ordinate: $\frac{d^2N}{dE.dw}$ particles/Gev. sterad. proton

Abscissa: Energy E, Mev

Figure 4.

Attenuation of neutrons (E_n < 20 Mev) and nucleons (E > 20 Mev) in concrete (ρ = 2350 kg/m^3).

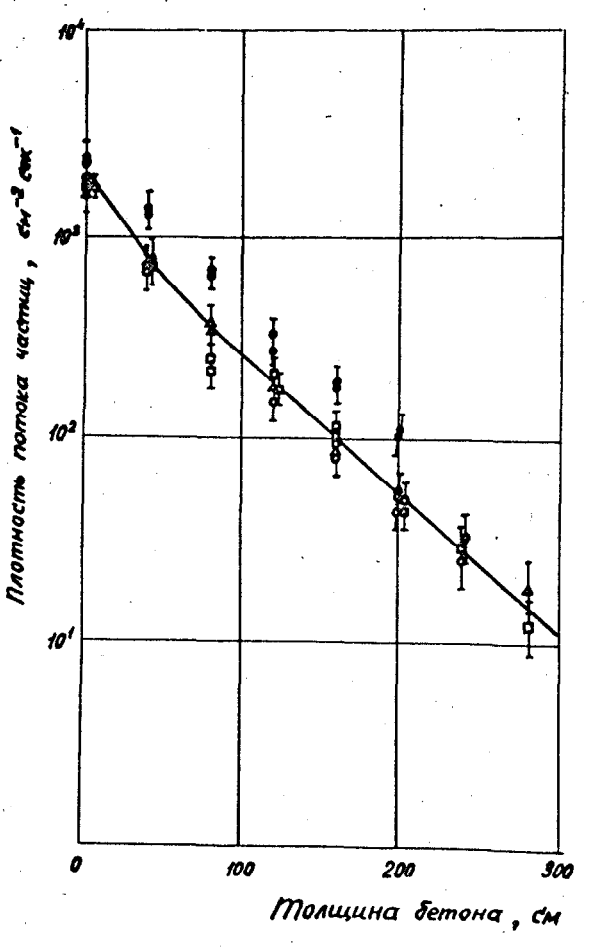

o, Δ, □ - nucleons when the energies of the primary protons are 10, 7, and 3.2 Gev respectively;

———— calculated curve;

● neutrons (E < 20 Mev) when the primary proton energy is 10 Gev.

Ordinate: particle flux density, $cm^{-2}sec^{-1}$

Abscissa: concrete thickness, cm.

Figure 5.

Density of neutron stars in a nuclear emulsion at various depths in concrete (ρ = 2350 kg/m^3).

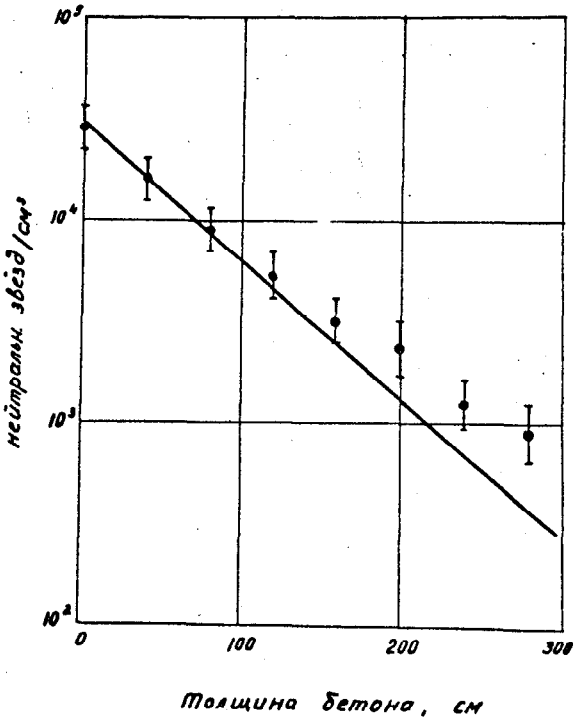

• experimental points (energy of primary protons = 10 Gev);

——— calculated curve.